SRC1 promotes Th17 differentiation by overriding Foxp3 suppression to stimulate RORγt activity in a PKC-θ–dependent manner

Subha Sen[a], Fei Wang[a], Jing Zhang[a,b], Zhiheng He[a], Jian Ma[a], Yousang Gwack[c], Jianming Xu[d], and Zuoming Sun[a,1]

[a]Division of Immunology, Beckman Research Institute of the City of Hope, Duarte, CA 91010; [b]Irell and Manella Graduate School of Biological Sciences, City of Hope, Duarte, CA 91010; [c]Department of Physiology, David Geffen School of Medicine, University of California, Los Angeles, CA 90095; and [d]Department of Molecular and Cellular Biology, Baylor College of Medicine, Houston, TX 77030

Edited by Philippa Marrack, National Jewish Health, Denver, CO, and approved November 20, 2017 (received for review October 24, 2017)

Th17 cells are major players in multiple autoimmune diseases and are developmentally contingent on reciprocal functionality between the transcription factor Retineic acid receptor-related orphan nuclear receptor gamma (RORγt) and Forkhead box protein P3 (Foxp3). Here we deciphered a previously unappreciated role of Steroid receptor coactivator 1 (SRC1) in defining the lineage decision for the development of Th17 versus induced T-regulatory (iTreg) cells. We demonstrate that SRC1 functions as a critical coactivator for RORγt in vivo to promote the functional dominance of RORγt over Foxp3 and thus establishing an unopposed Th17 differentiation program. In the absence of SRC1, T cell polarization resulted in decreased IL-17$^+$ and increased Foxp3$^+$ cells during both in vitro differentiation and in vivo development of experimental autoimmune encephalomyelitis. Mechanistically, T cell receptor (TCR) signaling molecule protein kinase C theta (PKC-θ)–mediated phosphorylation of SRC1 is important for inducing enhanced RORγt–SRC1 interaction, stable DNA binding, and resultant IL-17A transcription. Furthermore, phospho-SRC1–mediated recruitment of CARM1 induced prominent asymmetric dimethylation of H3R17 while preventing repressive H3K9 trimethylation and hence further modifying the IL-17 locus for optimal transcription. Moreover, binding of phospho-SRC1 to RORγt displaced bound Foxp3, leading to prompt degradation of the dissociated Foxp3 via a ubiquitin–proteosomal pathway and hence reversing the inhibitory action of Foxp3 on RORγt activity. Thus, SRC1 acts as a crucial molecular mediator to integrate positive PKC-θ–dependent TCR signals to induce peak RORγt activity and establish phenotypic dominance of Th17 over the iTreg pathway.

T cell differentiation | Th17 | Treg | EAE

Inflammatory Th17 cells and inhibitory Treg cells, which can be differentiated from the same pool of naive T cells (1, 2), determine the magnitude of immune responses. Skewing the balance toward Th17 cells could lead to aggravating autoimmunity, whereas tipping the balance toward Tregs induces tolerance (3). Generation of a robust Th17 response is essential for clearing pathogens and requires the differentiation and expansion of Th17 cells while reciprocally inhibiting the formation of Tregs. On the other hand, effective prevention of Th17-mediated autoimmunity requires the repression of Th17 while reciprocally promoting the formation of Treg cells. Th17 differentiation is directed by the master transcriptional factor RORγt, whereas Treg differentiation is instructed by the transcriptional repressor Foxp3. The initial differentiation phase of Th17 is marked by coexpressed RORγt and Foxp3 (4, 5). Foxp3 can bind directly to RORγt protein and antagonize its ability to bind DNA, thus exerting a negative effect on RORγt transcriptional activity (6, 7). However, it remains unclear exactly how RORγt can overcome Foxp3-mediated inhibition to promote the development of IL-17$^+$ cells.

The steroid receptor coactivator (SRC) family consists of three members, SRC1, SRC2, and SRC3. SRCs are important cofactors for steroid nuclear receptor-mediated transactivation, as SRC recruits acetyltransferases and methyltransferases that epigenetically modify histones to activate gene expression (8). Although SRCs do not directly bind to target DNA, SRCs are able to interact with transcription factors, including RORγt, to stimulate transcription (9). SRCs are thus believed to orchestrate transcription programs critical for multiple functions (8). However, the in vivo function of SRCs in the immune system remains unexplored.

Protein kinase C theta (PKC-θ) is significantly enriched in T cell compartments (10) and mediates critical costimulatory CD28 signals to regulate T cell activation and differentiation by association with CD28 (10–12). PKC-θ–deficient mice are resistant to T cell-mediated autoimmunity, including Th17-dependent experimental autoimmune encephalomyelitis (EAE), (13, 14) by inhibiting Th17 and promoting Treg differentiation (15, 16). However, the molecular mediators of PKC-θ–dependent costimulatory signals in the reciprocal regulation of IL-17$^+$ and Foxp3$^+$ cell differentiation are not known.

Modulation of RORγt activity by the associated cofactor SRC1 has been noted, but the mechanistic details of how it affects IL-17 transcriptional program and whether it can be controlled by T-cell signaling remained unknown. We demonstrate here that SRC1 is required to establish an unopposed Th17 program by inducing RORγt–SRC1–CARM1 complexes critical for epigenetically opening the IL-17 locus and by overriding Foxp3 inhibition via a PKC-θ–dependent phosphorylation event.

Significance

Poor understanding of the mechanisms responsible for the development of IL-17$^+$ and Foxp3$^+$ cells prevents the development of potent clinical treatments to boost protective Th17 immunity and repress the pathogenic Th17 responses that induce autoimmunity. Here we show that SRC1 phosphorylated by TCR signaling kinase PKC-θ functions as a coactivator in vivo to stimulate RORγt activity by disrupting the binding of inhibitory Foxp3 and induce Foxp3 degradation. SRC1 is thus an important checkpoint downstream of TCR signals to promote the dominance of RORγt over Foxp3 to establish an unopposed Th17 differentiation program. Our results thus provide a rationale for the development of SRC1-based treatments to control the scale of Th17 immunity by reciprocal shift of Th17 and T-regulatory cell differentiation.

Author contributions: S.S. and Z.S. designed research; S.S., F.W., J.Z., Z.H., and J.M. performed research; J.Z., Z.H., Y.G., and J.X. contributed new reagents/analytic tools; S.S. and Z.S. analyzed data; and S.S. and Z.S. wrote the paper.

The authors declare no conflict of interest.

This article is a PNAS Direct Submission.

[1]To whom correspondence should be addressed. Email: zsun@coh.org.

This article contains supporting information online at www.pnas.org/lookup/suppl/doi:10.1073/pnas.1717789115/-/DCSupplemental.

Results

Deletion of SRC1 Impairs IL-17$^+$ While Reciprocally Enhancing Foxp3$^+$ Cell Differentiation. Among the three SRC family members, overexpression (Fig. S1 *A–C*) or knockdown (Fig. S1 *D–F*) of SRC1 had most dramatic effects on the generation of IL-17$^+$ cells and genes (Fig. S1*G*) critical for Th17 differentiation, a finding supported by the presence of SRC1 in the RORγt immune complex as detected by mass spectrometry (Fig. S1*H*). *SRC1*$^{-/-}$ mice are generally normal, including splenic cellularity (Fig. S2*A*), CD4$^+$/CD8$^+$ T cell distribution in lymph nodes and spleen (Fig. S2*B*), and activation-induced T cell proliferation (Fig. S2*C*). Analysis of in vitro T cell differentiation did not detect defects in Th1 and Th2 differentiation of *SRC1*$^{-/-}$ CD4$^+$ T cells (Fig. S2 *D* and *E*). However, *SRC1*$^{-/-}$ CD4$^+$ T cells developed markedly fewer IL-17$^+$ cells and more Foxp3$^+$ cells ($P < 0.05$) (Fig. 1 *A* and *B*), which was also confirmed using highly purified naive CD4$^+$ T cells (Fig. S2 *F* and *G*). IL-6–mediated activation of Stat3 is critical for Th17 differentiation (17); however neither surface expression of the IL-6 receptor or gp130 (Fig. S2*H*) nor activation of Stat3 (Fig. S2*I*) of *SRC1*$^{-/-}$ T cells differed from WT cells. Surface T cell receptor (TCR) and CD28 levels were equivalent on *SRC1*$^{-/-}$ and WT T cells (Fig. S2*J*), suggesting that the impaired development of IL-17$^+$ cells from *SRC1*$^{-/-}$ T cells is not due to abnormal expression of TCR or dysregulated IL-6 signaling. Given that both IL-17$^+$ and Foxp3$^+$ cells can be differentiated from the same naive CD4$^+$ T cells, we monitored IL-17$^+$ and Foxp3$^+$ cells polarized under Th17 conditions (Fig. 1 *C* and *D*). Fewer IL-17$^+$ cells and more Foxp3$^+$ cells were detected in the *SRC1*$^{-/-}$ cell population than in the WT population. Interestingly, we did not observe an obvious difference in the percentage of WT and *SRC1*$^{-/-}$ Foxp3$^+$ cells among CD4$^+$CD25$^+$ cells stimulated by αCD3/αCD28 with or without Th17-priming cytokines (Fig. S2*K*). We thus focused on understanding SRC1 function in the reciprocal differentiation of IL-17$^+$ and Foxp3$^+$ cells under Th17-priming conditions. Deletion of SRC1 did not affect RORγt expression at the protein (Fig. 1 *E* and *F*) or mRNA level (Fig. S2*L*), despite markedly reduced expression of the Th17 signature genes *IL-17A*, *IL-17F*, *IL-23R*, *CCL20*, and *CCR6* (Fig. S2*L*). These results denote perturbation of RORγt

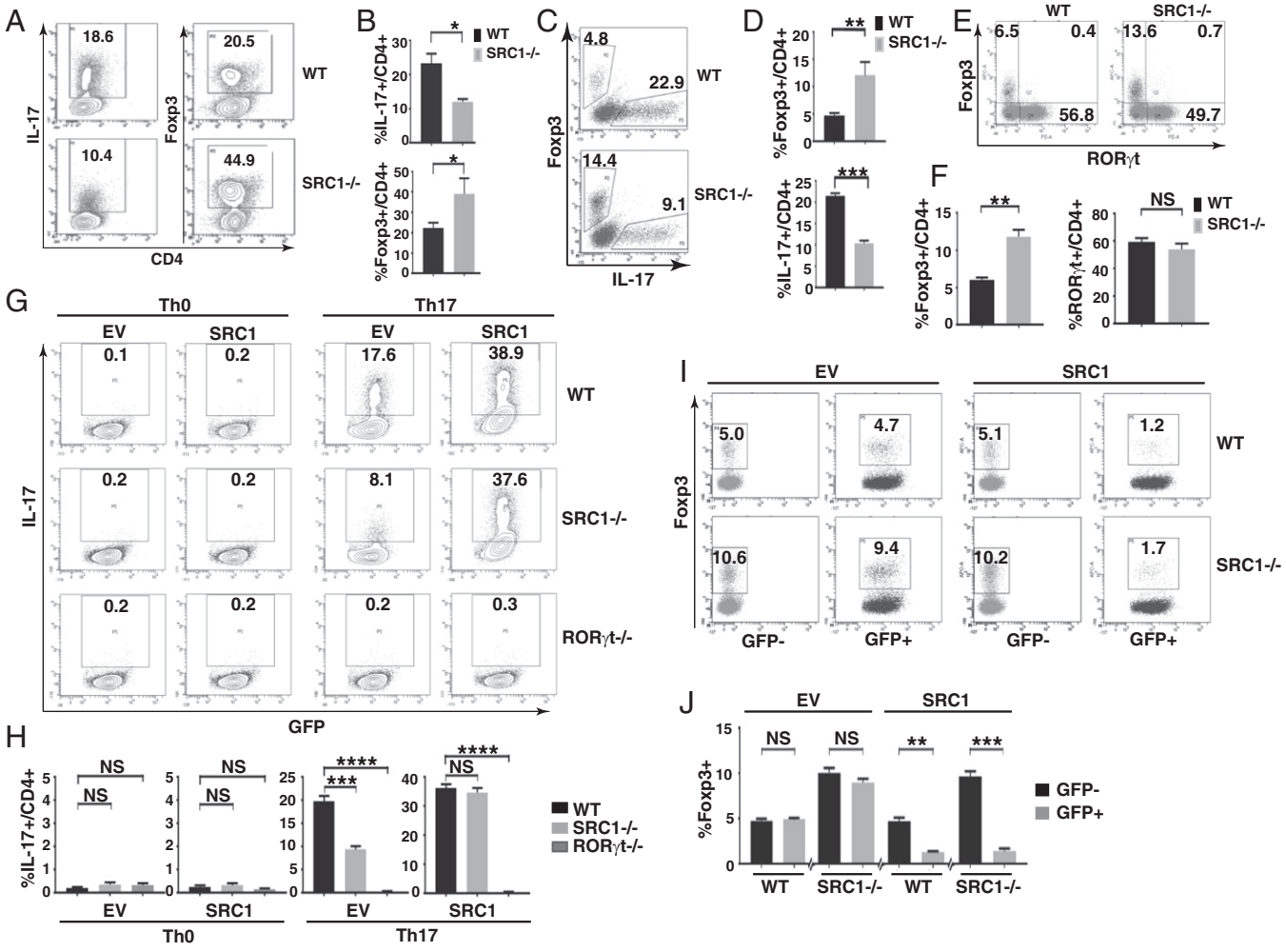

Fig. 1. SRC1 reciprocally regulates IL-17$^+$ and Foxp3$^+$ cell differentiation. (*A*) Flow cytometric analysis of the percentage of IL-17$^+$ or Foxp3$^+$ cells among WT or *SRC1*$^{-/-}$ CD4$^+$ T cells differentiated under Th17- or Treg-priming conditions for 3 d. (*B*) Quantification of the results shown in *A*. (*C*) Flow cytometric analysis of IL-17$^+$ and Foxp3$^+$ cells among WT or *SRC1*$^{-/-}$ CD4$^+$ T cells differentiated under Th17-priming conditions. (*D*) Quantification of the results shown in *C*. (*E*) Flow cytometric analysis of Foxp3 and RORγt among WT or *SRC1*$^{-/-}$ CD4$^+$ T cells differentiated under Th17-priming conditions. (*F*) Quantification of the results shown in *E*. (*G*) Flow cytometric analysis of IL-17$^+$ cells among indicated CD4$^+$ T cells transduced with control retrovirus expressing GFP alone (EV) or GFP with SRC1 and differentiated under Th0- or Th17-priming conditions. (*H*) Quantification of the results shown in *G*. (*I*) Flow cytometric analysis of Foxp3$^+$ cells among WT and *SRC1*$^{-/-}$ T cells transduced with control GFP$^+$ retrovirus only (EV) or with GFP together with SRC1 and differentiated under Th17-priming conditions. The percentage of Foxp3$^+$ cells among GFP$^-$ cells that were not transduced by retrovirus is also indicated. (*J*) Quantification of the results shown in *I*. Statistics are calculated based on three biological replicas. *$P < 0.05$, **$P < 0.01$, ***$P < 0.001$, ****$P < 0.0001$ (two-tailed unpaired *t* test in *B*, *D*, *F*, and *J*; one-way ANOVA with Tukey's post-analysis multiple-comparison test in *H*); NS, nonsignificant by unpaired *t* test. Error bars represent the SEM.

activity instead of RORγt expression in the absence of SRC1. Ectopic expression of RORγt in WT but not *SRC1*$^{-/-}$ CD4$^+$ T cells stimulated the generation of IL-17$^+$ cells (Fig. S2 *M* and *N*). Ectopic expression of SRC1 stimulated the generation of IL-17$^+$ cells in WT and *SRC1*$^{-/-}$ cells but not in RORγt$^{-/-}$ T cells, under Th17-priming but not under Th0-priming conditions (Fig. 1 *G* and *H*), although having equivalent amount of overexpressed SRC1 (Fig. S1*I*) in the GFP$^+$ population of the indicated strains of cells. SRC1 and RORγt thus depend on each other to regulate the differentiation of IL-17$^+$ cells. Moreover, overexpression of SRC1, but not of empty virus (EV), reduced the number of Foxp3$^+$ cells in both WT and *SRC1*$^{-/-}$ T cells under Th17-priming conditions (Fig. 1 *I* and *J*). These results thus indicate that SRC1, conjointly with RORγt, simultaneously promotes the differentiation of IL-17$^+$ cells and inhibits the formation of Foxp3$^+$ cells.

SRC1-Deficient Mice Are Resistant to EAE Associated with Decreased IL-17$^+$ and Increased Foxp3$^+$ Cells. The in vivo function of SRC1 was evaluated in the EAE model (18). Compared with an average peak clinical score of 3 for WT mice, the score of *SRC1*$^{-/-}$ mice was about 2, indicating significantly reduced EAE ($P < 0.01$) (Fig. 2*A*). Histological examination of spinal cords revealed less inflammation (H&E staining) and tissue damage due to demyelination (Luxol fast blue and FluoroMyelin Red staining) in *SRC1*$^{-/-}$ mice (Fig. S3 *A* and *B*). Impaired inflammation in *SRC1*$^{-/-}$ mice was indicated by significantly reduced CNS-infiltrating lymphocytes, including CD4$^+$ and CD8$^+$ T cells, Ly6G$^+$ monocytes, F4/80$^+$ macrophages, and CD19$^+$ B cells (Fig. S3 *C* and *D*). At the peak of the disease, WT and *SRC1*$^{-/-}$ mice showed equal percentages of CD4$^+$IFNγ$^+$ cells; however, *SRC1*$^{-/-}$ mice showed greatly reduced numbers of IL-17$^+$CD4$^+$ T cells ($P < 0.01$) (Fig. 2 *B* and *C*). Reduced production of IL-17A cytokine was observed in restimulated T cells from draining lymph nodes of immunized *SRC1*$^{-/-}$ mice (Fig. S3*E*). In contrast, the percentage of Foxp3$^+$ cell accumulation was markedly increased in *SRC1*$^{-/-}$ mice compared with WT mice (Fig. 2 *D* and *E*) during the recovery phase. Similarly, *Rag1*$^{-/-}$ hosts reconstituted with *SRC1*$^{-/-}$ CD4$^+$ T cells developed less severe EAE (Fig. S3*F*) together with reduced infiltrated IL-17$^+$ (Fig. S3 *G* and *H*) but increased Foxp3$^+$ cells (Fig. 3 *I* and *J*) compared with the *Rag1*$^{-/-}$ hosts reconstituted with WT CD4$^+$ T cells, demonstrating an intrinsic requirement for SRC1 in CD4$^+$ T differentiation. Therefore, SRC1 favors the conversion of CD4$^+$ T cells to IL-17$^+$ cells and not to Foxp3$^+$ cells in vivo during the development of EAE.

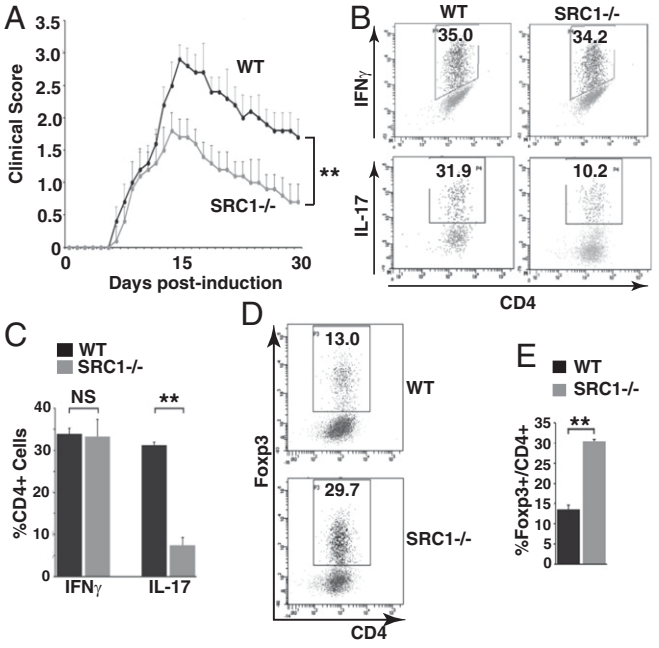

Fig. 2. *SRC1*$^{-/-}$ mice are resistant to EAE associated with reduced IL-17$^+$ and increased Foxp3$^+$ cells. (*A*) Mean EAE clinical score of indicated female mice at different days after immunization with MOG_{35-55}. (*B*) Flow cytometric analysis of the percentage of IFNγ$^+$ and IL-17$^+$ cells among infiltrated CD4$^+$ cells in the CNS of indicated EAE-induced mice. (*C*) Quantification of the results shown in *B*. (*D*) Flow cytometric analysis of the percentage of Foxp3$^+$ cells among infiltrated CD4$^+$ T cells in the CNS of the indicated EAE-induced mice. (*E*) Quantification of the results shown in *D*. $^{**}P < 0.01$ (nonparametric Mann–Whitney *u* test). NS, not significant.

SRC1 Regulates Reciprocal Differentiation of IL-17$^+$ and Foxp3$^+$ Cells in a PKC-θ–Dependent Manner. To explore how SRC1 and RORγt coregulate IL-17A transcription, we determined the effects of SRC1 and RORγt on the IL-17A promoter reporter. The expression of SRC1 in the presence of RORγt resulted in significantly increased reporter activity over that induced by RORγt alone, and the action was completely abrogated by a substitution mutation in the SRC1-binding motif of RORγt (RORγt-AF2) (Fig. S4*A*) (9). Interestingly, SRC1-mediated enhancement of RORγt activity was further amplified in the presence of phorbol 12-myristate 13-acetate (PMA) without a significant effect on RORγt alone (Fig. S4*A*). Since PMA is known to activate PKC, including PKC-θ, we examined whether stimulation with the anti-CD28 antibody, known to couple and activate intracellular PKC-θ (17), could produce a similar effect. Indeed, we found a CD28 dose-dependent increase in SRC1- and RORγt-mediated IL-17A reporter activity (Fig. S4*B*). These results are highly consistent with the observation in which *PKC-θ*$^{-/-}$ T cells show impaired Th17 differentiation (14, 15). Likewise, PMA treatment of in vitro differentiated WT, *SRC1*$^{-/-}$, and *PKC-θ*$^{-/-}$ T cells (Fig. 3 *A* and *B* and Fig. S4*C*) under Th17-priming conditions increased IL-17$^+$ cells and decreased Foxp3$^+$ cells in WT cells but not in the *PKC-θ*$^{-/-}$ or *SRC1*$^{-/-}$ T cell populations. The inability of PMA to affect the development of IL-17$^+$ and Foxp3$^+$ cells in *SRC1*$^{-/-}$ T cells indicates that SRC1 is downstream of PKC-θ in this process. This was reconfirmed by showing that forced expression of SRC1 increased IL-17$^+$ cells (Fig. 3 *C* and *E*) and decreased Foxp3$^+$ cells (Fig. 3 *D* and *F*) in a CD28 dose-dependent manner in GFP$^+$ compartments of Th17-primed WT cells but not in *PKC-θ*$^{-/-}$ T cells, even though the GFP$^+$ cells showed equivalent amounts of SRC1 (Fig. S4*D*). In contrast, nontransduced (GFP$^-$) cells or cells transduced with EV did not show any effect on the differentiation of IL-17$^+$ or Foxp3$^+$ cells. Together, these results demonstrate that SRC1 promotes IL-17$^+$ but inhibits Foxp3$^+$ cell development in a PKC-θ–dependent manner.

SRC1 Binding and Stimulation of RORγt Are Dependent on PKC-θ Catalytic Activity. To determine how PKC-θ regulates SRC1- and RORγt-mediated transactivation, we performed a RORγt-luciferase reporter assay in which SRC1-boosted RORγt transcriptional activity was further stimulated by the coexpression of constitutively active PKC-θ (C/A PKC-θ), but not by inactive PKC-θ (I/A PKC-θ), in a dose-dependent manner (Fig. 4*A*). Consistently, the SRC1–RORγt physical interaction was enhanced by active, but not inactive, PKC-θ in a dose-dependent manner (Fig. 4*B*), demonstrating that PKC-θ kinase activity is required for the SRC1–RORγt interaction. RORγt-AF2 is a mutant that does not bind SRC1, does not stimulate RORγt reporter and thus serves as a negative control. To understand whether RORγt DNA-binding ability is affected in presence of SRC1 and PKC-θ, we used band-shift analysis with an oligonucleotide probe containing the RORγt-binding site from the IL-17A promoter. Coexpression of RORγt and SRC1, having no intrinsic DNA-binding ability, markedly enhanced RORγt DNA-binding activity, as denoted by a higher-intensity RORγt–SRC1–DNA band clearly shifted from the lower-intensity basal RORγt–DNA band (Fig. 4*C*). Interestingly, in presence of active PKC-θ, but not inactive PKC-θ, RORγt–SRC1–DNA band intensity increased dose dependently with a simultaneous decrease of the RORγt–DNA band, denoting more pronounced RORγt DNA-binding activity in presence of SRC1 and active PKC-θ. Next, an endogenous RORγt–SRC1

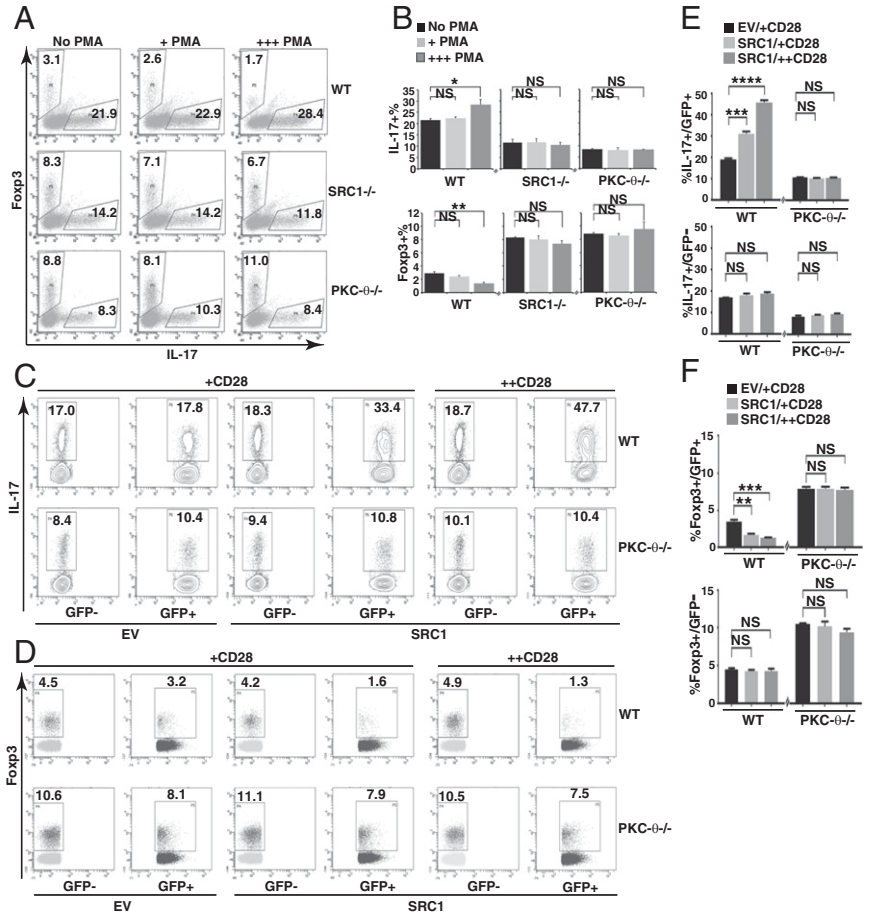

Fig. 3. SRC1 regulates reciprocal IL-17$^+$ and Foxp3$^+$ cell differentiation in a PKC-θ–dependent manner. (*A*) Flow cytometric analysis of IL-17$^+$ and Foxp3$^+$ cells among indicated CD4$^+$ T cells differentiated under Th17-priming conditions in the absence (no PMA) or presence of 1 nM PMA ($^+$PMA) or 10 nM PMA ($^{+++}$PMA) for 3 d. (*B*) Quantification of IL-17$^+$ and Foxp3$^+$ cells as shown in *A*. (*C*) Flow cytometric analysis of IL-17$^+$ cells among WT and *PKC-θ*$^{-/-}$ CD4$^+$ T cells transduced with virus expressing GFP (EV) or together with SRC1 and differentiated under Th17-priming conditions in the presence of 0.5 μg/mL ($^+$CD28) or 2.5 μg/mL ($^{++}$CD28) anti-CD28 antibody. Nontransduced GFP$^-$ cells are also shown. (*D*) Flow cytometric analysis of Foxp3$^+$ cells in cells shown in *C*. (*E*) Quantification of the results shown in *C*. (*F*) Quantification of the results shown in *D*. Statistics are calculated based on three biological replicates. NS, not significant; $*P < 0.05$, $**P < 0.01$, $***P < 0.001$, $****P < 0.0001$ (one-way ANOVA with Tukey's post-analysis multiple-comparison test).

interaction was detected by reciprocal immunoprecipitation with anti-RORγt or anti-SRC1 antibody in differentiated WT Th17 cells (Fig. 4*D*, *Left*); noticeably more RORγt–SRC1 complexes were detected in the presence of increasing CD28 stimulation, which activates PKC-θ. However, formation of RORγt–SRC1 complexes was minimal in *PKC-θ*$^{-/-}$ Th17 cells (Fig. 4*D*, *Right*), suggesting the critical function of PKC-θ in inducing the RORγt–SRC1 interaction in vivo. Taken together, our results demonstrate that a catalytically active form of PKC-θ is required to stimulate more pronounced SRC1 and RORγt interaction, which in turn promotes higher DNA-binding activity by RORγt and the subsequent transcriptional functionality.

Serines 1271 and 1272 of SRC1 Are Functional PKC-θ Phosphorylation Sites. Given that catalytically active, but not inactive, PKC-θ stimulates the coactivator properties of SRC1, we detected whether SRC1 was phosphorylated by using an antibody specific for phospho-Ser/Thr in a motif recognized by PKC. Indeed, phosphorylated SRC1 was detected in the presence of active, but not inactive, PKC-θ in a dose-dependent manner (Fig. S5*A*). Next, a stretch of seven phosphorylation serines or threonines (Fig. S5*B*) was identified in cells expressing active, but not inactive, PKC-θ by mass spectrometry. Although individual mutation of other phosphorylation sites to alanine had no effect, S1271A or S1271A significantly impaired the ability of SRC1 to bind and activate RORγt in the presence of active PKC-θ (Fig. S5 *C* and *D*) or to stimulate and rescue the differentiation of IL-17$^+$ cells in WT and *SRC1*$^{-/-}$ T cells, respectively (Fig. S5 *E* and *F*). Multiple sequence alignments showed these two phosphorylation sites to be highly conserved across different species (Fig. S5*G*), implying their potentially important function. Since single mutations at S1271 and S1272 only partially impaired SRC1 function, we next made double mutations, either S1271A/S1272A (SRC1^{AA}) or phosphomimetic mutations, S1271D/S1272D (SRC1^{DD}) and S1271E/S1272E (SRC1^{EE}). SRC1^{AA} failed to stimulate RORγt even in the presence of active PKC-θ, whereas SRC1^{DD} and SRC1^{EE} stimulated RORγt independently of active or inactive PKC-θ (Fig. S5*H*). As SRC1^{EE} was equivalent to SRC1^{DD}, only SRC1^{EE} was used for the rest of our studies. The overall increase in the structural stability of SRC1 (Fig. S5*I*), due to the replacement of serines by glutamic acid, as denoted by the in silico analysis, strongly suggests the importance of the phosphomodifications at S1271 and S1272 in the regulation of SRC1 functionality. Intriguingly, the computational analysis of sequence-based disorder prediction (Fig. S5*J*) denotes a higher probability of intrinsic disorder in the particular region of the SRC1 harboring the PKC-θ–targeted S1271A or S1272A residues (amino acids 1,261–1,310). Moreover, the disorder-enhanced phosphorylation site prediction (18) showed a high probability score for phosphorylation of S1271 and S1272 (Fig. S5*K*), further supporting the significance of our finding that these two sites are phosphor-modified

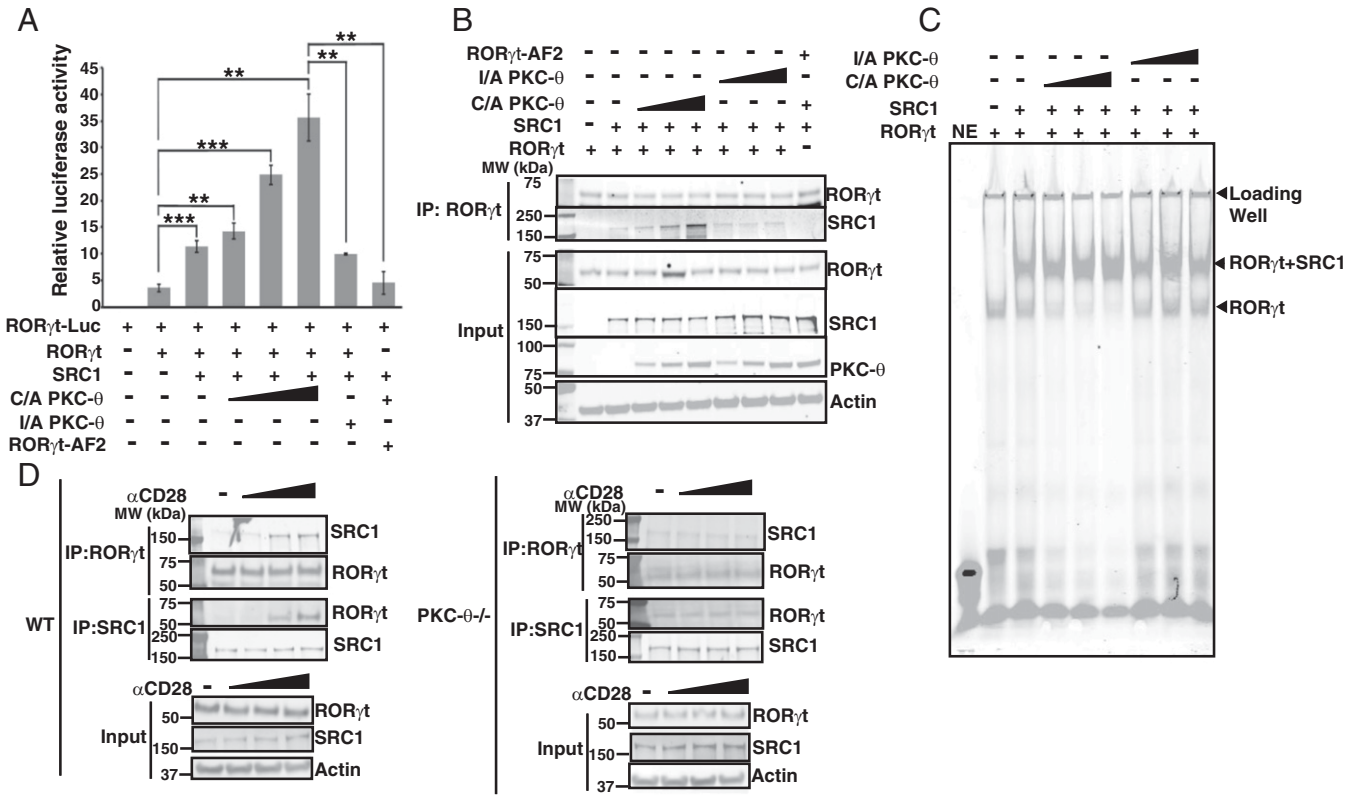

Fig. 4. SRC1 binds and activates RORγt in a PKC-θ–dependent manner. (*A*) Luciferase assay of RORγt reporter (RORγt-Luc) activity in HEK293T cells transfected with the indicated expression plasmids. The wedge indicates an increasing amount of the expression plasmid. The luciferase activity is normalized to Renilla luciferase activity (mean ± SD). $^{**}P < 0.01$, $^{***}P < 0.001$ (Student's two-tailed unpaired *t* test). (*B*) RORγt–SRC1 interaction in HEK293T cells transfected with the indicated expression plasmids, as determined by immunoprecipitation assay (IP). (*C*) RORγt and SRC1 complexes binding to a double-stranded oligonucleotide probe containing a RORγt-binding site, as detected by band-shift analysis with nuclear extracts prepared from HEK293T cells transfected with the indicated expression plasmids. NE, no nuclear extracts. (*D*) RORγt–SRC1 interaction in WT (*Left*) and *PKC-θ*$^{-/-}$ CD4$^+$ (*Right*) T cells unstimulated (–) or stimulated under Th17-priming conditions with increasing concentrations of anti-CD28 antibody (wedges), as determined by immunoprecipitation. *B*, *C*, and *D* are representatives of three independent experiments.

by PKC-θ. In the coimmunoprecipitation study, WT SRC interacted with RORγt in an active PKC-θ dose-dependent manner; SRC1^{AA} failed to interact with RORγt, even in the presence of active PKC-θ; and SRC1^{EE} bound to RORγt independent of active or inactive PKC-θ (Fig. 5*A*). Band-shift analysis also indicated that active PKC-θ stimulated the formation of RORγt–SRC1–DNA complexes in a dose-dependent manner but failed to stimulate the formation of RORγt–SRC1^{AA}–DNA complexes, whereas RORγt–SRC1^{EE}–DNA complexes were formed independently of active or inactive PKC-θ (Fig. 5*B*). WT SRC1, but not SRC1^{AA}, stimulated IL-17 reporter activity in a CD28-stimulation dose-dependent manner, whereas SRC1^{EE} stimulated IL-17 reporter activity independently of CD28 dosage (Fig. S5*L*). Therefore, the two identified PKC-θ–targeted phosphorylation sites of SRC1 are essential for stimulating peak RORγt activity by inducing maximal RORγt–SRC1 interaction, subsequent target DNA binding, and RORγt transcriptional ability.

Next, to determine the effect of SRC1 phosphorylation on the IL-17A locus conformation, we monitored histone acetylation [H3K(9)Ac, an active gene marker] at an RORγt-specific site on the IL-17 promoter (Fig. 5*C*) and the SRC1–RORγt interaction (Fig. S5*M*). *SRC1*$^{-/-}$ T cells reconstituted with EV and SRC1^{AA} had relatively low histone acetylation signals at the IL-17 locus (Fig. 5*C*, *Bottom*), which correlated with the lack of interaction between SRC1^{AA} and RORγt (Fig. S5*M*). In contrast, WT SRC1 increased H3K(9)Ac signals and SRC1–RORγt interaction in a CD28 dose-dependent manner, while SRC1^{EE} increased H3K(9)Ac signals and SRC1–RORγt interaction independent of CD28 dosage. Interestingly, SRC1^{AA} inhibited H3K(9)Ac signals in WT cells (Fig. 5*C*, *Top*) and thus behaved like a dominant negative SRC1. These results thus suggest enhanced IL-17 promoter accessibility marked with permissive histone modifications ensue in presence of phosphorylated SRC1. Finally, SRC1 and SRC1^{EE}, but not SRC1^{AA} expressed at the equivalent levels (Fig. S5*N*), promoted the development of IL-17$^+$ cells in both CD4$^+$ (Fig. 5 *D* and *E*) and highly purified naive CD4$^+$ WT and *SRC1*$^{-/-}$ T cells under Th17 priming (Fig. S5 *O* and *P*). Interestingly, only SRC1^{EE}, but not SRC1 or SRC1^{AA}, increased IL-17$^+$ cells in *PKC-θ*$^{-/-}$ T cells, further validating the function of PKC-θ–mediated phosphorylation of SRC1 in Th17 generation.

Phosphomodified SRC1 Recruits CARM1 to Optimally Activate IL-17 Gene Transcription. The critically important phosphorylation sites (S1271 and S1272) are located within the C-terminal activation domain 2 of SRC1, which is the known CARM1 (coactivator of arginine methyltransferase 1) interaction domain (19). This led us to speculate whether the phosphomodification of S1271 and S1272 of SRC1 could also affect the recruitment of CARM1, which in turn might affect the accessibility of the IL-17A locus for optimal transcription. Indeed, coexpression of RORγt, SRC1, and CARM1 led to significant increases in RORγt reporter activity compared with that induced by RORγt and SRC1 in presence of active PKC-θ (Fig. S6*A*). However, SRC1^{AA} failed to collaborate with CARM1 to activate the RORγt reporter in the presence of active PKC-θ, while the SRC1^{EE} synergizes with CARM1 to enhance RORγt in the presence of inactive PKC-θ. CARM1 possesses distinct histone methyltransferase activity to asymmetrically methylate the arginine17 residue of histone3, which

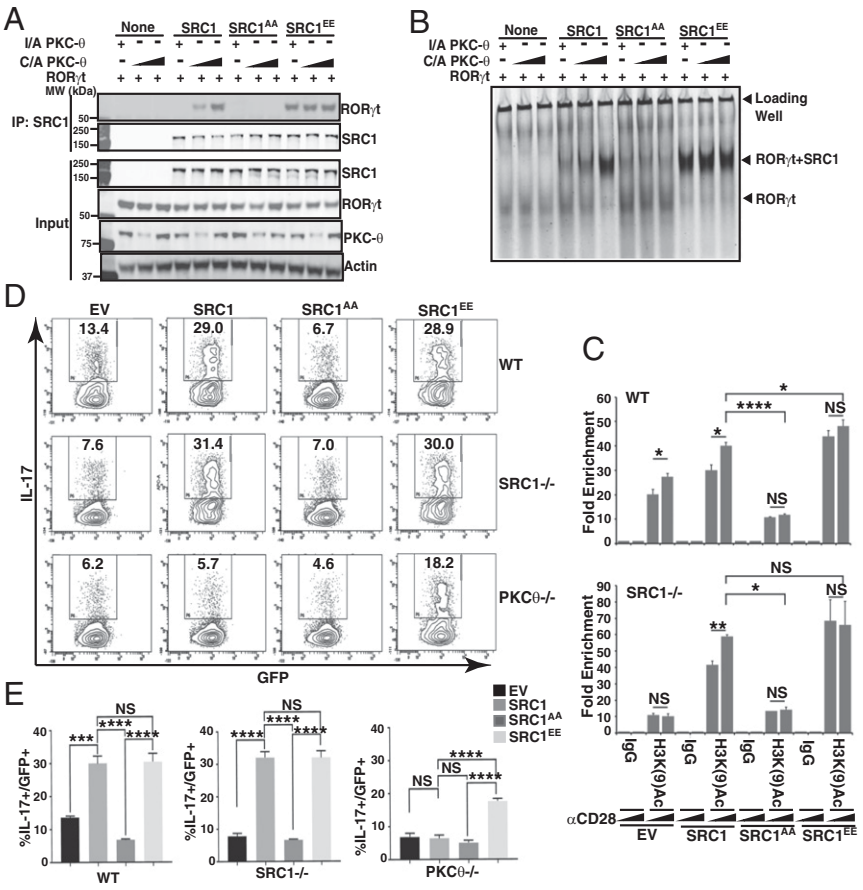

Fig. 5. Serines 1271 and 1272 of SRC1 are identified as functional PKC-θ phosphorylation sites. (*A*) Various SRC1–RORγt interactions in the presence and absence of two different doses of C/A PKC-θ or I/A PKC-θ in HEK293T cells transfected with the indicated expression plasmids, as determined by immunoprecipitation assay (IP). (*B*) Various SRC1–RORγt complexes binding to the RORγt-binding site, as detected by band-shift analysis with nuclear extracts prepared from HEK293T cells transfected with the indicated expression plasmids. (*C*) Histone acetylation [H3K(9)Ac] at the IL-17 promoter in WT (*Upper*) and *SRC1*$^{-/-}$ (*Lower*) CD4$^+$ T cells transduced with retrovirus expressing GFP alone (EV) or GFP together with SRC1 as indicated and differentiated under Th17-priming conditions in the presence of 0.5 μg/mL or 2.5 μg/mL of anti-CD28, as determined by ChIP assays with control IgG or anti-H3K(9)Ac antibody. Data are shown as mean ± SEM. (*D*) Flow cytometric analysis of IL-17$^+$ cells among WT, SRC1$^{-/-}$, and *PKC-θ*$^{-/-}$ CD4$^+$ T cells transduced with retrovirus expressing GFP alone (EV) or together with the indicated SRC1 and differentiated under Th17-priming conditions. (*E*) Quantification of the results shown in *D*. Statistics are calculated based on three biological replicates. NS, not significant; **P* < 0.05, ***P* < 0.01, ****P* < 0.001, *****P* < 0.0001 (Student's two-tailed unpaired *t* test in *C*; one-way ANOVA with Tukey's post-analysis multiple-comparison test in *E*) *A* and *B* are representatives of three independent experiments.

is primarily linked to gene activation in vivo (20, 21). We thus used a catalytic inactive form (E267Q) of CARM1 (22). In contrast to WT CARM1 (Fig. S6*A*), E267Q could not synergize with SRC1 to enhance the RORγt reporter (Fig. 6*A*). The significant reduction of the RORγt reporter by E267Q in the presence of SRC1^{EE} denotes that CARM1 is functionally downstream of SRC1, and its catalytic activity is required for optimal stimulation of RORγt activity.

ChIP with an anti-flag antibody was followed by immunoblotting from WT or *SRC1*$^{-/-}$ CD4$^+$ T cells differentiated under Th17 conditions and transduced with flag-tagged constructs of SRC1, SRC1^{AA}, SRC1^{EE}, or a C-terminal deletion of the CARM1-binding domain (SRC1-ΔAD2) (Fig. S6*B*). The protein complex pulled down along with SRC1 or SRC1^{EE} had both RORγt and CARM1 along with the distinct presence of H3R17a(me)2. When precipitated from cells transduced with either SRC1^{AA} or SRC1-ΔAD2, the recovery of RORγt was drastically reduced along with a remarkable loss of CARM1 protein and H3R17a(me)2 (Fig. S6*B*). These results thus point out that CARM1 recruitment and the resultant H3R17a(me)2 modification are critically dependent on the presence of phospho-SRC1. Similarly, the ChIP-qPCR assay detected the enrichment of CARM1 and H3R17a(me)2 at the promoters of the RORγt target genes IL-17A (Fig. 6*B*) and IL-23R (Fig. S6*C*) in WT cells but not in *SRC1*$^{-/-}$ CD4$^+$ T cells transduced with EV. Furthermore, CARM1 recruitment to the IL-17 or IL-23R loci and H3R17a(me)2 were enhanced by the ectopic expression of SRC1^{EE} but not SRC1^{AA} in both WT and *SRC1*$^{-/-}$ Th17 cells. Interestingly, the enrichment of CARM1 and H3R17a(me)2 reciprocally correlated with the repressive H3K9(me)3 modification at the IL-17 or IL-23R loci, which might denote a negative regulatory role of CARM1 toward this particular repressive H3K9(me)3 modification. These findings indicate that RORγt and SRC1, through recruitment of CARM1 to the IL-17A or IL-23R promoter, methylate histones to open the permissive chromatin structure while opposing repressive modification. Indeed, ectopic expression of CARM1 enhanced the production of IL-17A in WT CD4$^+$ T cells but failed to do so in *SRC1*$^{-/-}$ cells (Fig. 6 *C* and *D*), denoting SRC1-dependent corecruitment of CARM1 to the IL-17 locus. Furthermore, enzyme-dead CARM1-E267Q inhibited IL-17$^+$ differentiation in WT cells, revealing that enzymatic activity is required for modification of the target gene locus by CARM1. Likewise, knockdown of CARM1 impaired the generation IL-17$^+$ cells in WT but not in *SRC1*$^{-/-}$ T cells (Fig. S6 *D* and *E*). Collectively, these results demonstrate that phospho-SRC1 plays a dual positive role in promoting the Th17 transcription program by directly up-regulating RORγt activity and recruiting CARM1 to generate permissive H3R17a(me)2 while concurrently suppressing inhibitory H3K9(me)3 modification, thus rendering an overall active chromatin structure at critical Th17 gene loci.

Phosphorylation of SRC1 Overcomes Foxp3-Mediated Inhibition of RORγt to Promote Th17 Differentiation. Foxp3 suppressed RORγt-mediated IL-17A promoter activation by a physical interaction (6, 7). Consistent with previous observations, Foxp3 inhibited RORγt reporter activity, which remained unaltered even in the presence of SRC1 (Fig. S7*A*). However, SRC1 together with active, but not inactive, PKC-θ overcame the Foxp3-mediated inhibition and activated the RORγt reporter in a dose-dependent manner. The mutant RORγt-AF2, which cannot bind SRC1, failed to overcome Foxp3 inhibition even in the presence of active PKC-θ and SRC1, indicating that the recruitment of phospho-SRC1 has an essential role in the suppression of Foxp3 inhibition. In the coimmunoprecipitation assay, RORγt predominantly interacted with Foxp3 when both Foxp3 and SRC1 were present (Fig. S7*B*). However, with increasing amounts of active, but not inactive, PKC-θ, the RORγt–Foxp3 interaction diminished, and a more prominent RORγt–SRC1 interaction was detected, suggesting that the PKC-θ–induced

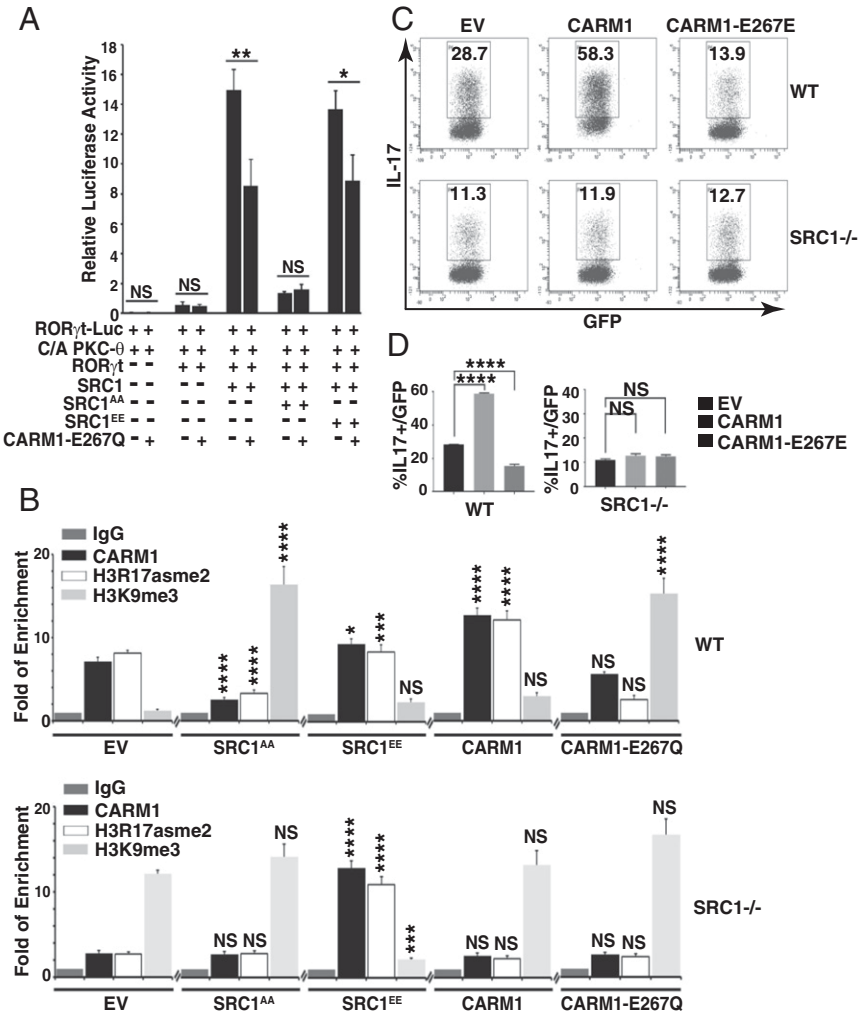

Fig. 6. Phosphorylated SRC1 recruits CARM1 to optimally activate IL-17 gene transcription. (*A*) Luciferase assay of the RORγt reporter in HEK293T cells transfected with the indicated expression plasmids. Data are normalized to Renilla luciferase activity (mean ± SD). (*B*) ChIP analysis of the enrichment of CARM1, H3R17asme2, and H3K9me3 in the IL-17A promoter region in GFP$^+$ fractions of WT and *SRC1*$^{-/-}$ CD4$^+$ T cells transduced with retrovirus expressing the indicated constructs or empty virus (EV), and differentiated under Th17-polarizing conditions. Results are presented as fold induction over IgG control. Data are representative of two independent experiments with three replicates per experiment (mean and SEM). (*C*) Flow cytometric analysis of IL-17$^+$ cells among WT or *SRC1*$^{-/-}$ CD4$^+$ T cells transduced with retrovirus expressing CARM1or CARM1-E267Q and cultured under Th17-priming conditions. (*D*) Quantification of the results shown in *C*. Data are shown as the mean and SEM of three experiments. NS, not significant; *$P < 0.05$, **$P < 0.01$, ***$P < 0.001$, ****$P < 0.0001$ (one-way ANOVA with Tukey's post-analysis multiple-comparison test).

heightened association of SRC1 with RORγt disrupts the Foxp3-RORγt interaction. Band-shift analysis also showed reduced RORγt–target DNA interaction as a result of increasing amounts of Foxp3 (Fig. S7*C*), which explains the inhibition of RORγt activity by Foxp3 (Fig. S7*A*). In presence of SRC1, RORγt, and Foxp3, only weak signals of RORγt–SRC1 complexes were detected. However, increasing active, but not inactive, PKC-θ restored the formation of RORγt–SRC1–DNA complexes in a dose-dependent manner, despite the presence of Foxp3, confirming the reversal of Foxp3 inhibition on RORγt DNA-binding activity. Consistently, SRC1^{EE}, but not SRC1^{AA}, reverted the Foxp3-mediated inhibition of RORγt activity, as substantiated by luciferase reporter activity (Fig. 7*A* and Fig. S7*D*), coimmunoprecipitation assays of the SRC1–RORγt interaction (Fig. 7*B*), and gel-shift assays of SRC1–RORγt–DNA complexes (Fig. 7*C*).

Foxp3 binds to RORγt to inhibit the differentiation of IL-17$^+$ cells (6, 7). Given that phosphorylated SRC1 can overcome the Foxp3-mediated inhibition of RORγt activity by dissociating the Foxp3–RORγt interaction (Fig. 7 *A*–*C*), we tested whether phosphorylation of SRC1 can overcome the Foxp3-inhibited differentiation of IL-17$^+$ cells. For this purpose, both Foxp3 (Thy1.1) and SRC1 (GFP) were retrovirally transduced into CD4$^+$ T cells (Fig. 7 *D* and *E*). Differentiation of IL-17$^+$ cells was not obviously affected in cells negative for both Foxp3 and SRC1 (GFP$^-$Thy1.1$^-$) but was inhibited in cells overexpressing Foxp3 (GFP$^-$Thy1.1$^+$). IL-17$^+$ cell differentiation was stimulated by SRC1 and SRC1^{EE}, but not by SRC1^{AA}, in cells expressing only SRC1 (GFP$^+$Thy1.1$^-$). In cells expressing both Foxp3 and SRC1 (GFP$^+$Thy1.1$^+$), inhibition of IL-17$^+$ cell differentiation was induced by Foxp3 (GFP Thy1.1 vs. GFP Foxp3/Thy1.1); this inhibition was overcome by SRC1 (SRC1/GFP, Foxp3/Thy1.1) and SRC1^{EE} (SRC1^{EE}/GFP, Foxp3/Thy1.1) but not SRC1^{AA} (SRC1^{AA}/GFP, Foxp3/Thy1.1). Collectively, we demonstrate the mechanisms by which phosphorylated SRC1 overrides the Foxp3-mediated inhibition of RORγt transcriptional activity to maximally induce Th17 differentiation.

To further answer how, despite having unchanged mRNA levels, *SRC1*$^{-/-}$ T cells differentiated in vitro under Th17-polarizing conditions accumulate a higher amount of Foxp3 protein than WT Th17 cells (Fig. 1*E* and Fig. S2*L*), we considered the possibility that SRC1 might be involved in the regulation of Foxp3 protein stability. Furthermore, under similar conditions, *PKC-θ*$^{-/-}$ T cells showed detectably higher levels of Foxp3$^+$ cells, and the level was only reduced by phosphomimetic SRC1^{EE} but not SRC1 or SRC1^{AA}, reaffirming the role of PKC-θ–phosphorylated SRC1 in reducing the Foxp3 protein level in differentiating Th17 cells. We monitored Foxp3 levels in the presence and absence of MG132, which inhibits proteasome-dependent degradation. Foxp3 was below the detectable level in WT CD4$^+$ T cells differentiated under Th17 conditions (Fig. 8*A*, *Upper*), which is consistent with the observation of fewer Foxp3$^+$ cells under this condition (Fig. 1*C*). However, a low level of Foxp3 protein was detected in the presence of MG132, suggesting that blockade of the proteasomal pathway accumulates detectable Foxp3 and implicating the involvement of proteosomal degradation of Foxp3 in Th17 cells. As Foxp3 is susceptible to ubiquitination-induced degradation (23, 24), we monitored the ubiquitination of Foxp3 (Fig. 8*B*, *Upper*). Tandem ubiquitin-binding entity (TUBE) beads (25) were used to enrich ubiquitinated

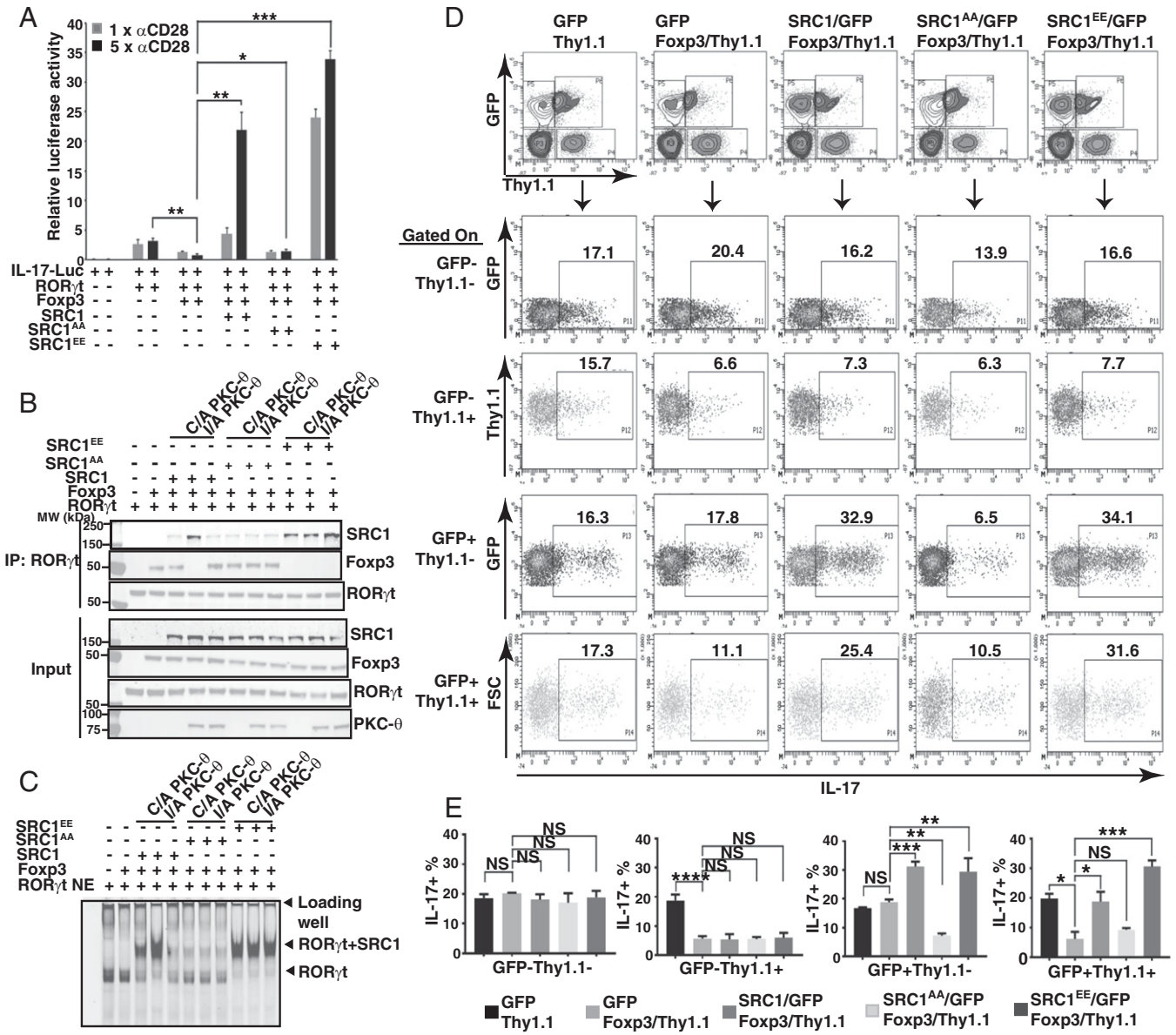

Fig. 7. Phosphorylated SRC1 overcomes Foxp3-mediated inhibition of RORγt to promote Th17 differentiation. (*A*) Luciferase assay of the RORγt reporter in HEK293T cells transfected with indicated expression plasmids and normalized to that of Renilla luciferase (mean ± SD). (*B*) RORγt–SRC1 and RORγt–Foxp3 interactions in HEK293T cells transfected with the indicated expression plasmids, as determined by immunoprecipitation. (*C*) SRC1–RORγt complexes binding to the RORγt-binding site, as detected by band-shift analysis with nuclear extracts prepared from HEK293T cells transfected with the indicated expression plasmids. NE, no nuclear extracts. (*D*) Flow cytometric analysis of IL-17$^+$ cells among CD4$^+$ T cells transduced by retrovirus expressing GFP alone (GFP) or GFP together with the indicated SRC1 and retrovirus expressing Thy1.1 alone or together with Foxp3 and differentiated under Th17-priming conditions. (*E*) Quantification of the results shown in *D*. NS, not significant; *$P < 0.05$, **$P < 0.01$, ***$P < 0.001$, ****$P < 0.0001$ (Student's two-tailed unpaired *t* test; one-way ANOVA-with Tukey's post-analysis multiple-comparison test in *E*). *B* and *C* are representatives of three independent experiments.

proteins. Ubiquitination of Foxp3 was detected in MG132-treated cells with TUBE beads but not with control beads. In contrast to WT cells, Foxp3 was detectably higher in *SRC1*$^{-/-}$ T cells even without MG132, which correlated with reduced the Foxp3 ubiquitination level in these cells supporting the stabilization of Foxp3. These results suggest that in Th17 cells SRC1 promotes Foxp3 degradation via an ubiquitination-dependent proteasomal pathway. Decreased Foxp3 levels accompanied with increased ubiquitination in WT or *SRC1*$^{-/-}$ T cells expressing SRC1^{EE}, but not SRC1^{AA}, further verify the specific requirement of phospho-SRC1 for Foxp3 degradation. Previous studies have shown that the E3 ligase Stub1 is responsible for the ubiquitination of Foxp3 for degradation (23). Indeed, knockdown of Stub1 impaired Foxp3 ubiquitination and stabilized Foxp3 in WT cells, with limited effect in *SRC1*$^{-/-}$ T cells (Fig. S7*E*). Finally, differentiating Th17 cells overexpressing either SRC1 or SRC1^{EE}, but not SRC1^{AA}, in CD4$^+$ (Fig. 8 *C* and *D*) or highly purified naive CD4$^+$ (Fig. S7 *F* and *G*) WT and *SRC1*$^{-/-}$ T cells showed reduced accumulation of Foxp3$^+$ cells. Furthermore, under similar conditions, *PKC-θ*$^{-/-}$ T cells showed detectably higher levels of Foxp3$^+$ cells, and the level was only reduced by phosphomimetic SRC1^{EE} while SRC1 but not SRC1^{AA}, reaffirming the role of PKC-θ–phosphorylated SRC1 in reducing the Foxp3 protein level in differentiating Th17 cells. Therefore, phospho-SRC1, by displacing Foxp3 and redirecting it for proteosomal degradation, frees up the RORγt-dependent Th17 programming, thus exerting a reciprocal effect on IL-17$^+$ and Foxp3$^+$ cell differentiation.

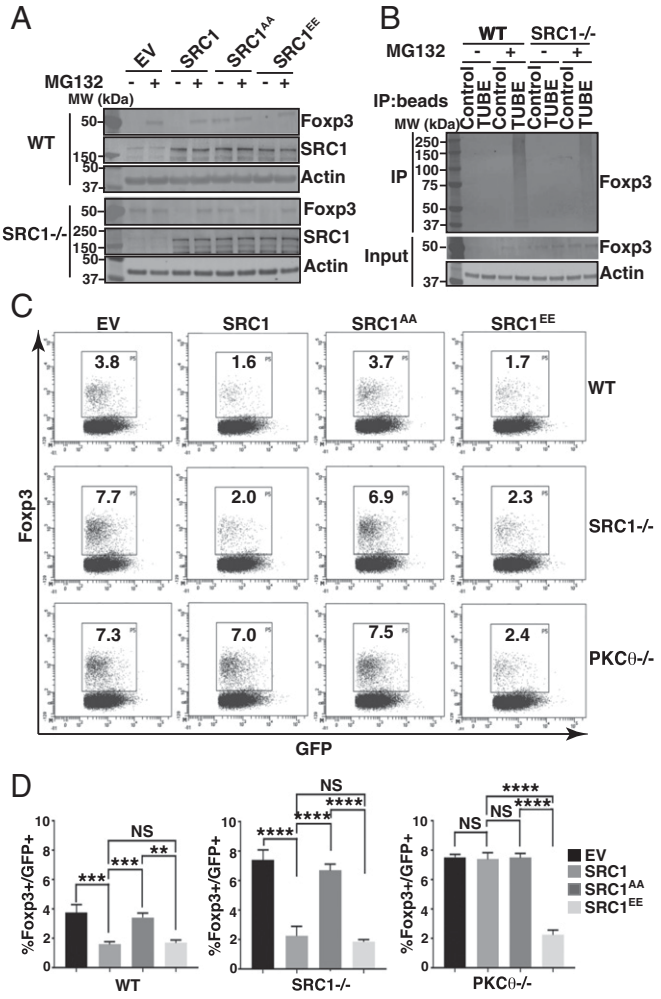

Fig. 8. (*A*) Foxp3 levels in WT (*Upper*) and *SRC1*$^{-/-}$ (*Lower*) CD4$^+$ T cells transduced by retrovirus expressing the indicated SRC1 and differentiated under Th17-priming conditions, followed by treatment with or without 20 μg MG132 for 3 h, as determined by immunoblots. (*B*) Foxp3 levels and ubiquitination in WT and *SRC1*$^{-/-}$ CD4$^+$ T cells differentiated under Th17-priming conditions for 3 d, followed by treatment with or without 20 μg MG132 for 3 h, as detected by immunoblot. Ubiquitination is detected after ubiquitinated proteins in cell lysates are enriched by control or TUBE beads. (*C*) Flow cytometric analysis of Foxp3$^+$ cells in the indicated CD4$^+$ cells transduced with retrovirus expressing GFP alone or GFP together with the indicated SRC1 and differentiated under Th17-priming conditions. (*D*) Quantification of the results shown in *C*. NS, not significant; $^{**}P < 0.01$, $^{***}P < 0.001$, $^{****}P < 0.0001$ (one-way ANOVA with Tukey's post-analysis multiple-comparison test). Data in *A* and *B* are representative of three independent experiments.

Discussion

Our results demonstrate multiple events occurring either concurrently or sequentially during the Th17 developmental pathway: (*i*) Phosphorylation induced higher interaction of phospho-SRC1 with RORγt, leading to increased cognate DNA-binding activity of RORγt and resultant transcriptional activity of IL-17A. (*ii*) Concurrent with the binding of phospho-SRC1, Foxp3 is released from RORγt and subsequently is degraded via the ubiquitin–proteosomal pathway, thus inverting the Foxp3-mediated suppression of RORγt. (*iii*) Phospho-SRC1 specifically recruits the histone methyl transferase CARM1 to deposit active mark, H3R17 asymmetric dimethylation, at IL-17 locus, which in turn prevents repressive chromatin modification of H3K9 trimethylation. (*iv*) Consequently, the IL-17A locus is stabilized by higher H3K9 acetylation, leading to amplified IL-17A transcription and marked phenotypic dominance/stability of the Th17 lineage.

CD28 costimulation favors the development of IL-17$^+$ but not Foxp3$^+$ cells (26, 27). Consistent with its being an important CD28 signaling molecule, PKC-θ promotes the development of IL-17$^+$ but inhibits the differentiation of Foxp3$^+$ cells (14–16). While differentiation of IL-17$^+$ and Foxp3$^+$ cells is controlled by RORγt and Foxp3, respectively, it was not clear how these transcriptional factors sense CD28 signals to reciprocally regulate IL-17$^+$ and Foxp3$^+$ differentiation. We demonstrate here that the CD28 signaling molecule PKC-θ is the downstream sensor that coordinates RORγt and Foxp3 activity via phosphorylation of coactivator SRC1. In response to CD28 costimulation, PKC-θ mediates the phosphorylation of two conserved serines (1271 and 1272) in SRC1. Notably, the overall increase in the structural stability of SRC1 due to phosphomodification of the two serines and the higher probability score for phosphorylation of S1271 and S1272, as denoted by the computational analysis and further verified by empirical loss- and gain-of-function studies, collectively signify the physiological importance of these phosphomodifications in the regulation of SRC1 functionality in the T cell context.

Both RORγt and Foxp3 expression can be induced in the same T cells, and RORγt$^+$Foxp3$^+$ double-positive cells are detected in vivo (6, 7, 28). The final fate of these double-positive cells is controlled by the balance between RORγt and Foxp3 activity. SRC1 exerts dual actions on these two opposing transcription factors to leverage the action of one over the other. Our results indeed demonstrate that PKC-θ–mediated phosphomodification of SRC1 eventuates the release of bound Foxp3 from RORγt, either due to conformational change or steric constraints or through competitive binding. The displaced Foxp3 is subsequently degraded via the ubiquitination pathway, resulting in uninhibited stimulation of IL-17$^+$ differentiation with reciprocal attenuation of Foxp3-mediated differentiation. We show that Foxp3 is degraded via a previously known (23) STUB1-dependent ubiquitination and proteosomal pathway. As evidenced before (23), the absence of Stub1 in differentiated T cells under Th17-skewing culture conditions increased Foxp3 expression relative to controls. This implies that in normally differentiating Th17 cells the accumulation of Foxp3 is prevented by prompt proteosomal degradation mediated by Stub1. Our study thus provides the mechanistic basis for how Foxp3 is dissociated and/or simultaneously prevented from association with RORγt and hence is directed to Stub1-mediated proteosomal degradation. Besides, it has also been shown that inflammatory cytokines such as IL1β promote Foxp3 degradation via the Stub1-dependent pathway (23). Therefore, it is possible that IL1β, being present in the micromilieu of developing Th17 cells in vivo, might provide the degradation signal by acting through IL-1R, a direct target of RORγt. It is possible that phosphorylated SRC1 promotes IL-1β–induced Foxp3 degradation by stimulating RORγt-dependent IL-1R expression; this could be an interesting topic for future investigation.

Multiple transcription factors have been shown to regulate the development of IL-17$^+$ and Foxp3$^+$ cells (29). While we could not find any change in the binding pattern of IRF4, BATF, or RUNX1 to RORγt complexes in the absence of SRC1 (Fig. S7*H*), further analysis of SRC1-interacting transcription factors and their target genes will facilitate a better understanding of how SRC1 orchestrates these transcription factors to regulate reciprocal Th17 and Treg differentiation at a genome-wide level. SRC1 inhibitors have been developed to treat cancer (8, 30). SRC1 inhibitors are expected to relieve Th17-mediated autoimmunity by both decreasing Th17 and increasing Treg cells simultaneously. Therefore, our study provides the rationale for the development of SRC1-based treatments.

Experimental Procedures

Mice. All animal experiments were performed in specific pathogen-free facilities in the Beckman Research Institute, City of Hope following national, state, and institutional guidelines. Animal protocols were approved by the

Institutional Animal Care and Use Committee at the Beckman Research Institute, City of Hope.

T Cell Differentiation. Naive or total $CD4^+$ T cells were purified using model-based analysis for ChIP-sequencing (MACS) and a FACSAria III cell sorter before stimulation with anti-CD3/CD28 antibodies (0.5 and 0.5 μg/mL, respectively) in a 24-well plate (BioLegend) for 2–3 d. Th17-skewing conditions consisted of Iscove's modified Dulbecco's medium (IMDM) supplemented with 10% FBS, 20 ng/mL IL-6, 2.5 ng/mL TGFβ (PeproTech), and 5 ug/mL neutralizing antibodies against IFNγ and IL-4 (BioLegend).

qRT-PCR. Total RNA was isolated using the RNeasy Isolation Kit according to the manufacturer's instructions (Qiagen). cDNA was synthesized with the SuperScript III First-Strand Synthesis system (Invitrogen), and real-time PCR was performed on a Bio-Rad iCycler thermal cycler with SsoFast SYBR Green Supermix (Bio-Rad). mRNA levels were determined by the comparative critical threshold (CT) method and normalized to β-actin expression.

EAE Induction. Six- to eight-week-old, sex-matched WT and *SRC1*$^{-/-}$ littermates were injected s.c in the rear flank with 100 μg MOG35–55 peptide (2HN-MEVGWYRSPFSRVVHLYRNGK-COOH) in complete Freund's adjuvant (Sigma), and 250 ng pertussis toxin (List Biological) was injected i.p. Mice were monitored daily, and disease severity was scored.

Immunoprecipitation and Western Blotting. Immunoprecipitation and Western blotting were performed as we previously described (31, 32). Immunoprecipitations were done using a Pierce Crosslink IP kit and clean-Blot IP detection system (Thermo Scientific).

Reporter Gene Assays. The luciferase reporter gene assay reagents were obtained from Promega, and the assay was performed per the manufacturer's instructions.

EMSA. Essentially similar to the technique described previously (33), IR800 infrared dye-labeled complementary oligos (Integrated DNA Technologies) were used for EMSA. EMSA was performed with an Odyssey Infrared EMSA kit. Nuclear extracts were harvested with the Nuclear Extract Kit (Active Motif).

ChIP Assays. ChIP analysis was carried out according to the manufacturer's protocol (Upstate/Millipore). The amount of immunoprecipitated DNA was quantified by real-time PCR with the ABI PRISM 7500 Sequence Detection System (Applied Biosystems) using SYBR Green.

TUBE Pull-Down. Detection of ubiquitinated proteins from $CD4^+$ T cells was done as described in ref. 32. Cell lysates were incubated with Agarose-TUBE2 (LifeSensors) or control beads at 4 °C for 4 h. After washing, beads were suspended in SDS reducing sample buffer. Eluted samples were analyzed by Western blotting.

Computational Analysis. Prediction of protein stability changes upon single point mutation from the protein sequence (NP_035011.1) was done using i-Mutant2.0 (folding.biofold.org/i-mutant/i-mutant2.0.html). Prediction of intrinsic protein disorder, domain, and globularity was done by GlobPlot 2 (globplot.embl.de/). The analysis of disorder-potentiated phosphorylation site prediction was done with DisPhos 1.3 (www.dabi.temple.edu/disphos/pred.html).

Statistical Analysis. An unpaired Student's *t* test was used to determine significance ($*P < 0.05$).

ACKNOWLEDGMENTS. We thank Dr. Liang Zhou (University of Florida) for the MIG-Thy1.1 plasmids and Dr. Kenneth J. Dery, Dr. Ramakrishna Chandran, and Dr. Maciej Kujawski (City of Hope) for providing critical advice for gel-shift analysis, EAE, and IL-17 ELISA, respectively. This work was supported by NIH Grants R01-AI053147 and R01-AI109644, a California Institute of Technology–City of Hope Cancer Center Pilot Project Support Grant, a University of California, Riverside–City of Hope Biomedical Initiatives Excellence Award, and the National Cancer Institute of the NIH under Award P30CA33572, which includes work performed in the animal, genomic, flow cytometry, anatomic pathology, and mass spectrometric cores supported by this grant. The content is solely the responsibility of the authors and does not necessarily represent the official views of the NIH.

1. Hoechst B, Gamrekelashvili J, Manns MP, Greten TF, Korangy F (2011) Plasticity of human Th17 cells and iTregs is orchestrated by different subsets of myeloid cells. *Blood* 117:6532–6541.
2. Komatsu N, et al. (2014) Pathogenic conversion of Foxp3+ T cells into TH17 cells in autoimmune arthritis. *Nat Med* 20:62–68.
3. Langrish CL, et al. (2005) IL-23 drives a pathogenic T cell population that induces autoimmune inflammation. *J Exp Med* 201:233–240.
4. Veldhoen M, Hocking RJ, Atkins CJ, Locksley RM, Stockinger B (2006) TGFbeta in the context of an inflammatory cytokine milieu supports de novo differentiation of IL-17-producing T cells. *Immunity* 24:179–189.
5. Yang XO, et al. (2008) Molecular antagonism and plasticity of regulatory and inflammatory T cell programs. *Immunity* 29:44–56.
6. Zhou L, et al. (2008) TGF-beta-induced Foxp3 inhibits T(H)17 cell differentiation by antagonizing RORgammat function. *Nature* 453:236–240.
7. Ichiyama K, et al. (2008) Foxp3 inhibits RORgammat-mediated IL-17A mRNA transcription through direct interaction with RORgammat. *J Biol Chem* 283:17003–17008.
8. Walsh CA, Qin L, Tien JC, Young LS, Xu J (2012) The function of steroid receptor coactivator-1 in normal tissues and cancer. *Int J Biol Sci* 8:470–485.
9. Xie H, Sadim MS, Sun Z (2005) RORgammat recruits steroid receptor coactivators to ensure thymocyte survival. *J Immunol* 175:3800–3809.
10. Sun Z (2012) Intervention of PKC-θ as an immunosuppressive regimen. *Front Immunol* 3:225.
11. Sun Z, et al. (2000) PKC-theta is required for TCR-induced NF-kappaB activation in mature but not immature T lymphocytes. *Nature* 404:402–407.
12. Isakov N, Altman A (2012) PKC-theta-mediated signal delivery from the TCR/CD28 surface receptors. *Front Immunol* 3:273.
13. Anderson K, et al. (2006) Mice deficient in PKC theta demonstrate impaired in vivo T cell activation and protection from T cell-mediated inflammatory diseases. *Autoimmunity* 39:469–478.
14. Tan SL, et al. (2006) Resistance to experimental autoimmune encephalomyelitis and impaired IL-17 production in protein kinase C theta-deficient mice. *J Immunol* 176:2872–2879.
15. Kwon MJ, Ma J, Ding Y, Wang R, Sun Z (2012) Protein kinase C-θ promotes Th17 differentiation via upregulation of Stat3. *J Immunol* 188:5887–5897.
16. Ma J, Ding Y, Fang X, Wang R, Sun Z (2012) Protein kinase C-θ inhibits inducible regulatory T cell differentiation via an AKT-Foxo1/3a-dependent pathway. *J Immunol* 188:5337–5347.
17. Kong KF, et al. (2011) A motif in the V3 domain of the kinase PKC-θ determines its localization in the immunological synapse and functions in T cells via association with CD28. *Nat Immunol* 12:1105–1112.
18. Iakoucheva LM, et al. (2004) The importance of intrinsic disorder for protein phosphorylation. *Nucleic Acids Res* 32:1037–1049.
19. Chen D, et al. (1999) Regulation of transcription by a protein methyltransferase. *Science* 284:2174–2177.
20. Bauer UM, Daujat S, Nielsen SJ, Nightingale K, Kouzarides T (2002) Methylation at arginine 17 of histone H3 is linked to gene activation. *EMBO Rep* 3:39–44.
21. Wu J, Xu W (2012) Histone H3R17me2a mark recruits human RNA polymerase-associated factor 1 complex to activate transcription. *Proc Natl Acad Sci USA* 109:5675–5680.
22. Lee YH, Koh SS, Zhang X, Cheng X, Stallcup MR (2002) Synergy among nuclear receptor coactivators: Selective requirement for protein methyltransferase and acetyltransferase activities. *Mol Cell Biol* 22:3621–3632.
23. Chen Z, et al. (2013) The ubiquitin ligase Stub1 negatively modulates regulatory T cell suppressive activity by promoting degradation of the transcription factor Foxp3. *Immunity* 39:272–285.
24. Kondo Y, et al. (1999) Beta-catenin accumulation and mutation of exon 3 of the beta-catenin gene in hepatocellular carcinoma. *Jpn J Cancer Res* 90:1301–1309.
25. Hjerpe R, et al. (2009) Efficient protection and isolation of ubiquitylated proteins using tandem ubiquitin-binding entities. *EMBO Rep* 10:1250–1258.
26. Korn T, Bettelli E, Oukka M, Kuchroo VK (2009) IL-17 and Th17 Cells. *Annu Rev Immunol* 27:485–517.
27. Semple K, et al. (2011) Strong CD28 costimulation suppresses induction of regulatory T cells from naive precursors through Lck signaling. *Blood* 117:3096–3103.
28. Lochner M, et al. (2008) In vivo equilibrium of proinflammatory IL-17+ and regulatory IL-10+ Foxp3+ RORgamma t+ T cells. *J Exp Med* 205:1381–1393.
29. Gaffen SL, Jain R, Garg AV, Cua DJ (2014) The IL-23-IL-17 immune axis: From mechanisms to therapeutic testing. *Nat Rev Immunol* 14:585–600.
30. Wang Y, et al. (2014) Bufalin is a potent small-molecule inhibitor of the steroid receptor coactivators SRC-3 and SRC-1. *Cancer Res* 74:1506–1517.
31. He Z, et al. (2017) A two-amino-acid substitution in the transcription factor RORγt disrupts its function in TH17 differentiation but not in thymocyte development. *Nat Immunol* 18:1128–1138.
32. He Z, et al. (2016) Ubiquitination of RORγt at lysine 446 limits Th17 differentiation by controlling coactivator recruitment. *J Immunol* 197:1148–1158.
33. Minch KJ, et al. (2015) The DNA-binding network of Mycobacterium tuberculosis. *Nat Commun* 6:5829.